Supplementary information

1. Identification of Specimens

Systematic Paleontology

Aves

Jeholornithiformes

Jeholornis sp.

Material: STM2-51, a slab and counter-slab preserving a nearly complete articulated specimen preserving ovarian follicles.

Locality and horizon: Early Cretaceous Yixian Formation, Jehol Group, Chaoyang, Liaoning, northeastern China.

Aves

Ornithothoraces

Enantiornithes

Enantiornithes indet.

Material: STM29-8, a slab and counter-slab preserving a nearly complete and articulated adult specimen preserving ovarian follicles and feather impressions; STM10-45, a slab and counter-slab preserving a nearly complete articulated subadult specimen preserving ovarian follicles.

Locality and horizon: STM29-8 is from the Early Cretaceous Jiufotang Formation, Toudaoyingzi, Jianchang, Liaoning, northeastern China; STM10-45 is from the Early Cretaceous Jiufotang Formation, Chaoyang, Liaoning, northeastern China.

Identification of specimens

Although parts of the skeleton are poorly preserved, STM2-51 can be confidently assigned to *Jeholornis* sp. Based on the following features: large size; elongate boney tail formed by more than 20 free caudal vertebrae; dorsoventrally deep skull; proximally straight ulna; carpometacarpus with large intermetacarpal space formed by caudal curvature of the minor metacarpal; three large, recurved claws on the hand; and tarsometatarsus proportionately short. The poor preservation of the skull prevents observation of the dental characters that would identify it at the species level.

Specimens STM29-8 and STM10-45 can both be assigned to Enantiornithes by the presence of: a minor metacarpal that extends distally farther than the major metacarpal; proximally forked and distally tapered pygostyle; distinct profile of humeral head, rising dorsally and ventrally from central concavity; incomplete fusion of the tarsometatarsus; and large and recurved pedal claws. The two specimens clearly represent different taxa, however preservation does not allow the specimens to be confidently assigned to a species.

STM29-8 is distinguishable from STM10-45 based on the following morphologies: coracoid, lateral margin very convex; narrow rostrum; femur < tibiotarsus; ulna > humerus; alular digit ending level with the distal end of the major metacarpal; and pedal digit II robust. The skull in

the main slab of STM29-8 appears to be tampered; amorphous black material fills the skull region with only the rostral end of the dentary and premaxilla preserving clear information. The general shape of the skull is considered genuine; in the counter-slab, although no morphologies are clear, the voids of the hyoid bones are clearly preserved ventral to the mandibular bones indicating that the basis for the skull is legitimate. Still, we include no information from the skull in this paper.

STM10-45 is distinguishable from STM29-8 based on the following features: femur and tibiotarsus subequal; lateral margin of coracoid concave with rudimentary lateral process present; furcular rami slightly bowed; scapular acromion robust and mediolaterally expanded; humerus, ulna subequal; alular digit short, not reaching distal end of major metacarpal; manual claws small; and pedal digit II robust.

STM 10-45 is considered a subadult based on the incomplete fusion of compound bones (carpometacarpus, tibiotarsus, and tarsometatarsus). STM29-8 is considered more mature based on the greater degree of fusion in these bones, although preservation prevents determining the exact degree of fusion in both specimens.

2. Additional figures of specimens preserving ovaries

Figure S1. Counter-slab of *Jeholornis* sp. STM2-51 in ventral view. Scale bar equals one centimeter.

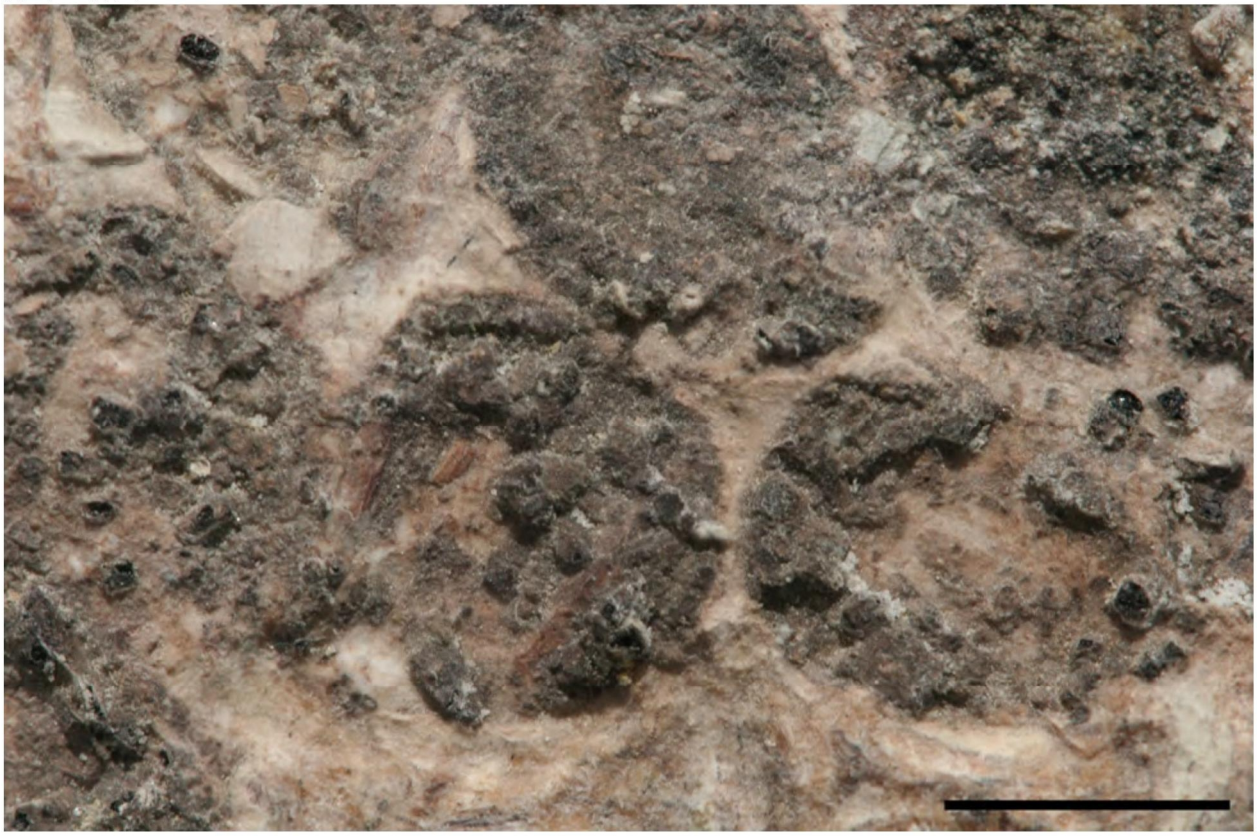

Figure S2. Close up photograph of follicles in *Jeholornis* sp. STM2-51. Scale bar equals one centimeter.

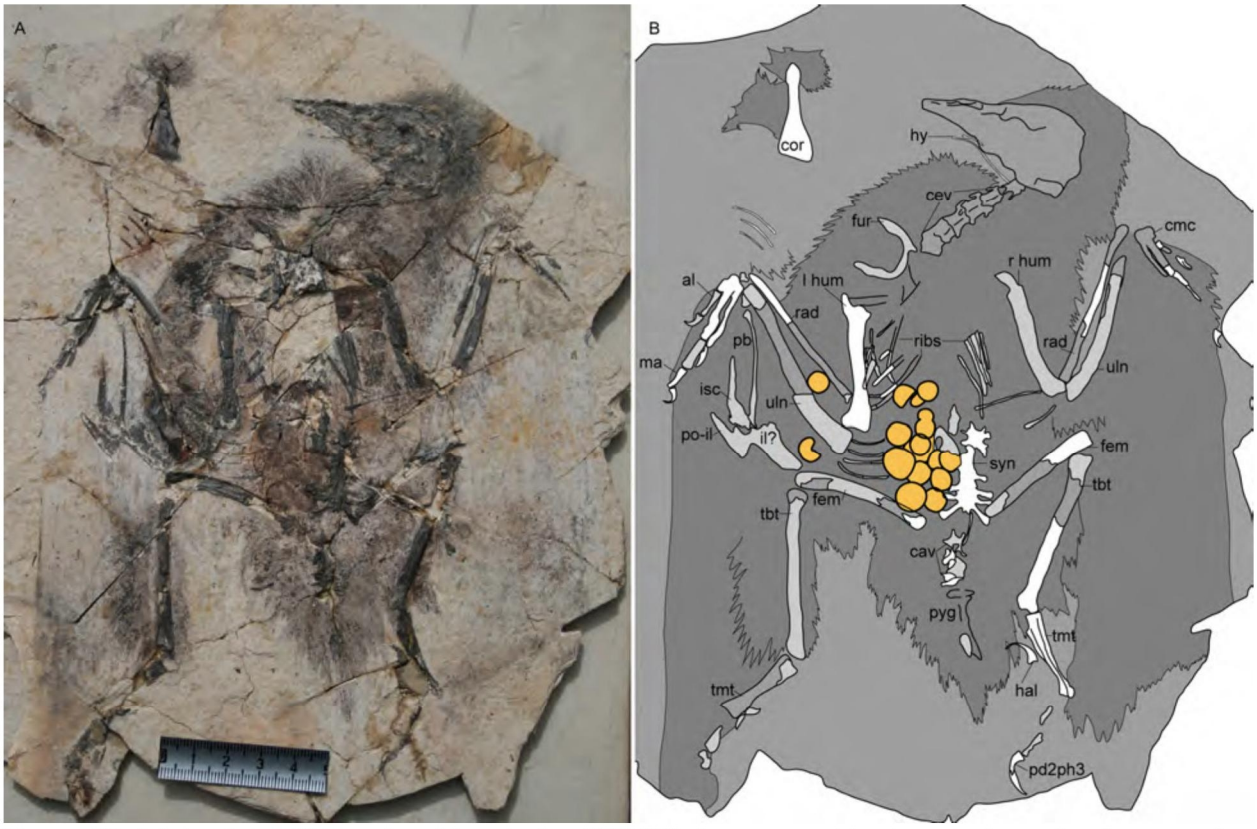

Figure S3. Main slab of Enantiornithes indet. STM29-8 preserved in dorsal view: A, photograph; B, camera lucida drawing. Anatomical abbreviations: **al**, alular digit; **cav**, caudal vertebrae; **cev**, cervical vertebrae; **cmc**, carpometacarpus; **cor**, coracoid; **fem**, femur; **fur**, furcula; **hal**, hallucal claw; **hy**, hyoid bones; **il?**, ilium?; **ma**, major digit; **pb**, pubis; **pd2ph3**, pedal digit two third phalanx (ungual); **po-il**, post-acetabular ilium; **pyg**, pygostyle; **rad**, radius; **sca**, scapula; **syn**, synsacrum; **tbt**, tibiotarsus; **tmt**, tarsometatarsus; **uln**, ulna. Scale bar equals one centimeter. Well-preserved bone is indicated by white; light grey indicates poorly preserved bone; medium grey indicates matrix; dark grey indicates feather impressions; follicles are indicated by yellow.

Figure S4. Photograph of the counter-slab of Enantiornithes indet. STM29-8 (ventral view). Scale bar equals one centimeter. Area marked by the red dashed line may be slightly tampered.

Figure S5. Close up photograph of the follicles in Enantiornithes indet. STM29-8. Scale bar equals one centimeter.

Figure S6. Counter-slab of Enantiornithes indet. STM10-45 (ventral view): A, photograph; B, interpretative drawing. Anatomical abbreviations not in Figure S3: **alm**, alular metacarpal; **den**, dentary; **mac**, major metacarpal; **mic**, minor metacarpal; **mt**, metatarsals; **pc**, proximal carpal; **pmx**, premaxilla; **sc**, semilunate carpal; **stn**, sternum. Scale bar equals one centimeter.

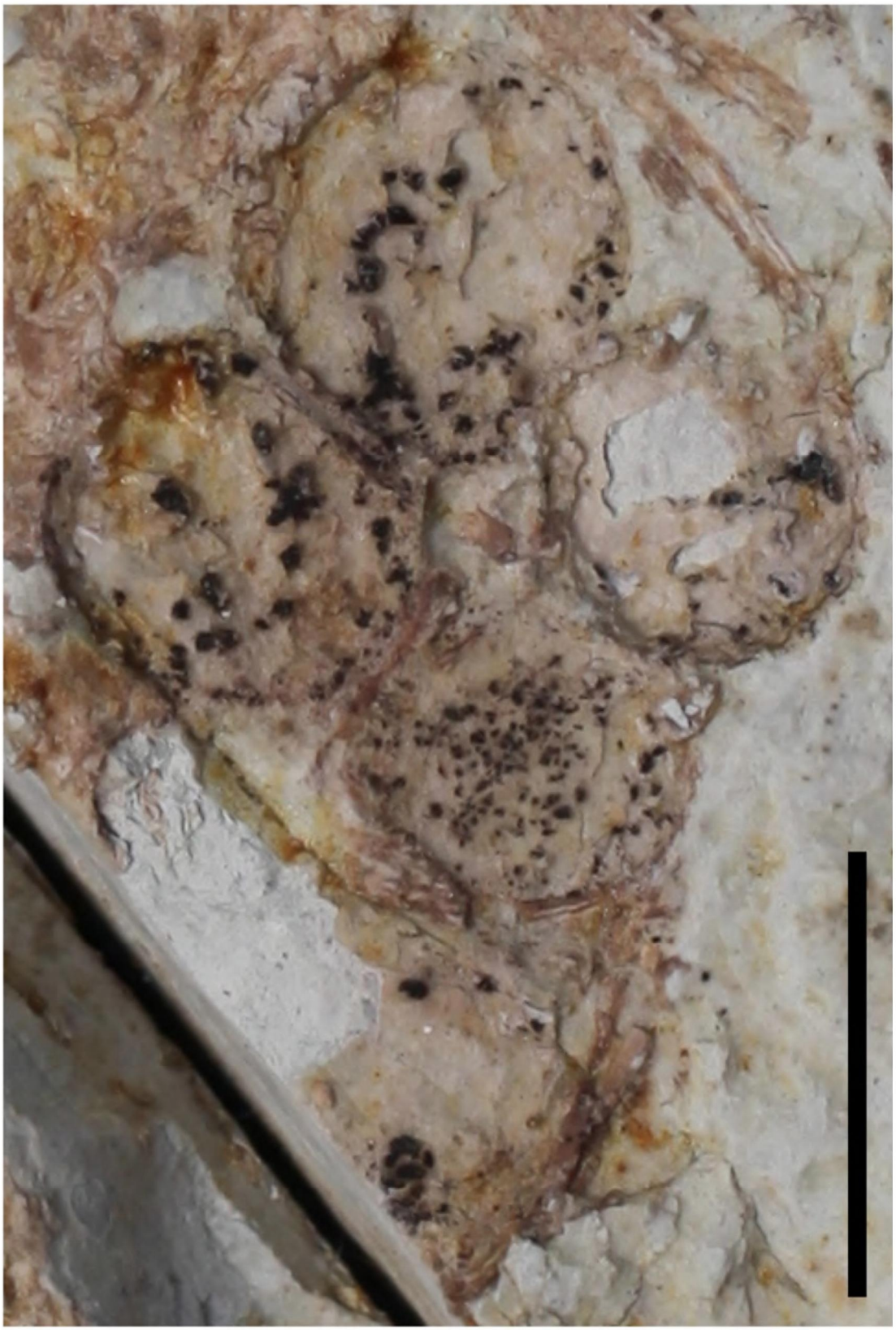

Figure S7. Close up photograph of the follicles in the counter-slab of Enantiornithes indet. STM10-45. Scale bar equals one centimeter.

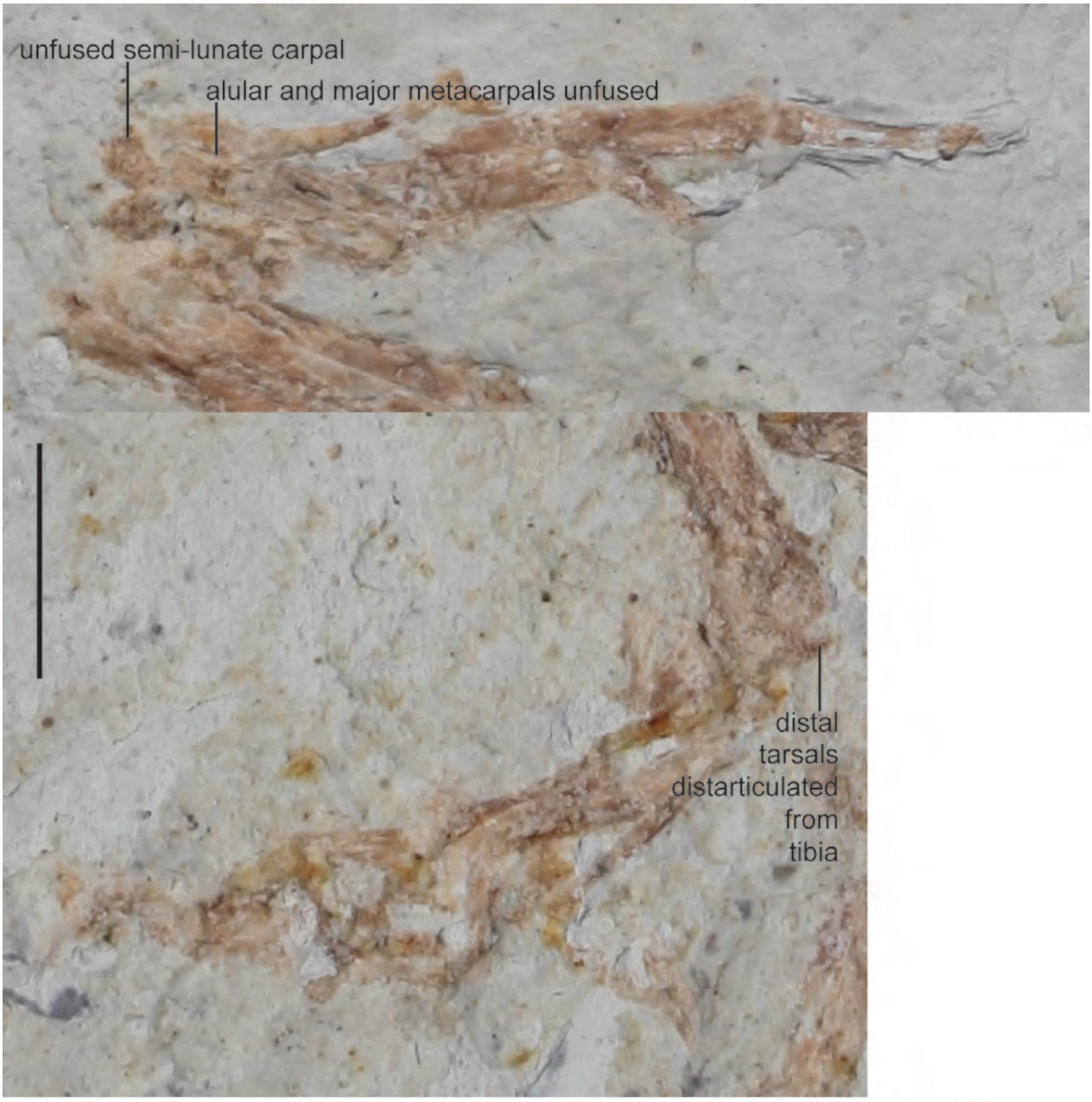

Figure S8. A, Close up of the left carpometacarpus from the counter-slab of enantiornithine STM10-45 showing the lack of fusion between the carpal and metacarpal bones; B, close up of the distal right tibiotarsus and foot showing absence of fusion. Scale bar equals one centimeter.

3. Preservation

The differential preservation of soft-tissue among Jehol vertebrates is poorly understood[30]. Furthermore, the type of preservation differs in each of the specimens reported here (e.g. mineral composition of the bone, as inferred by color; STM29-8 preserves integument while STM10-45 preserves none) – the only shared feature is the overall poor quality of the bone preservation, badly crushed in the three specimens. The follicles are consistent in size and position but otherwise are preserved differently; they are crystallized in STM2-51, preserved as impressions in STM10-45, and as carbon in STM29-8. Overall In anoxic environments, preservation of soft

tissue is a race against decay by anaerobic bacteria[31], however partial preservation of soft tissue, where ph and chemical composition were favorable, is known to occur [32,33]. Biological structures with greater resistance to decay due to chemical structure or otherwise, most commonly animal cuticles, have a greater chance of preservation[34]; the outer membranes of the ovarian follicles may have served to protect the oocyte long enough for their structure to be preserved. The follicle is actually the composite of the developing germ cell (the primary oocyte) and the deposited yolk contained in a sac, which ruptures when ovulation occurs so that the oocyte alone travels into the oviduct. The developing follicle is encased in a highly vascularized perifollicular membrane and a well-developed network of blood vessels[7]. Mature ova also have a perivitelline layer, formed by a three-dimensional network of non-collagenous structural connective proteins responsible for preventing intraspecific insemination[7]. Immature oocytes are not encased in a sac and further lack the membranes present in primary oocytes, which may explain why these structures were not preserved.

While it is unclear why certain structures preserve in some specimens but not others, enantiornithine STM29-8 also preserves uncinate processes, a small structure on the rib present in modern birds but also known to occur in non-avian maniraptorans, Confuciusornithiformes, and basal ornithuromorphs[35]. This structure has previously been strangely undocumented in Enantiornithes, not preserved in a single specimen (reported in *Longipteryx* but ribs are fragmented and disarticulated and interpretations are equivocal)[8]. The fact they are preserved here suggests that the peculiar taphonomic processes that led to the preservation of the follicles may also have led to the preservation of these structures that are typically lost. The rare preservation of uncinate processes suggests that they remain cartilaginous in this clade.

4. Follicle Measurements

The follicles were measured as the average of two distinct diameter measurements, oriented at 90˚ when possible.

Table S1. Follicle measurements.

Specimen	Number of follicles	Follicle diameter (mm), range	Average diameter (mm)	Standard deviation
Jeholornis sp. STM2-51	~18-20	6.7-8.79	7.65	0.527
Enantiornithes indet. STM29-8	~14	5.83-8.83	6.86	0.908
Enantiornithes indet. STM10-45	~5-7	6.72-8.78	7.56	0.920

5. Body Mass Estimates

Mass was estimated from humerus length using the equations provided by Liu et al. (2012). See Table 1 for measurements and estimates.

Table S2. Select measurements and body masses.

	Femur length (mm)	Humerus length (mm)	Body mass (g)
Jeholornis sp. STM2-51	88.072	118.3	676.45
Enantiornithes indet. STM29-8	40.248	44.77	125.56
Enantiornithes indet. STM10-45	31.524	40.43	105.2

6. Histological Analysis

We conducted histological analysis on the three specimens in order to determine if medullary bone also formed in enantiornithine birds and *Jeholornis*, as it does in some ovulating dinosaurs, confuciusornithiforms, and living birds (absent in crocodilians)[16, 17,36]. Bone samples were taken from all three specimens; only a single sample could be retrieved from STM10-45 and it could not be used for histological analysis. Two samples were taken from each of the other specimens, as close to midshaft as preservation allowed: the ulna and femur were sampled in STM2-51 and the humerus and femur were sampled in STM29-8. The samples were taken using a micro-saw and were embedded in EXAKT Technovit 7200 one-component resin and allowed to dry for 24 hours. The samples were then cut and polished until the desired optical contrast was reached. The samples were viewed under normal and polarized light using a Leica DM-RX polarizing microscope.

Results

STM2-51

Ulna. The thin section of the ulna (SFig. 9A) displays three distinct regions: an inner poorly vascularized region of more parallel-fibered bone tissue (inner circumferential layer, ICL) with osteocyte lacunae arranged in parallel; a thick middle region of more woven-textured bone tissue with plump, haphazardly organized osteocyte lacunae; and an outer region (outer circumferential layer, OCL) of more parallel-fibered bone tissue with osteocyte lacunae that are flatter and arranged in parallel (SFig. 9A). The outer region is marked by several rest lines (four – six). The middle region of the compacta is richly vascularized and there appears to be a predominance of longitudinally and reticular oriented vascular channels. Isolated secondary osteons are visible. A double line of arrested growth (LAGs) appears to interrupt this region very close to the outer, more parallel fibered region. Such double LAGs are occasionally observed in dinosaurs[37] but frequently observed in frogs[38]. The medullary surface is broken; no medullary bone can be identified.

Femur. The thin section of the femur (SFig. 9B) reveals three distinct regions in the bone compacta: an inner poorly vascularized region of more parallel-fibered bone tissue with osteocyte lacunae arranged in parallel (ICL); a thick middle region of more woven-textured bone tissue with plump, haphazardly organized osteocyte lacunae; and an outer region (OCL) of more parallel-fibered bone tissue with osteocyte lacunae that are flatter and arranged in parallel. The outer region is marked by one LAG and at least one rest line. The middle region of the compacta is more richly vascularized than the ulna but the vascular channels appear to have less of an overall longitudinal orientation compared to the ulna (more reticular). Fewer secondary osteons are visible compared to the thin section of the ulna. The inner layer is very poorly preserved and

potentially diagenetically altered although faint osteocyte lacunae are still visible. The inner surface of the medullary cavity is broken and no medullary bone can be identified.

STM29-8

Humerus. The thin section of the enantiornithine humerus displays three distinct regions: an inner poorly vascularized region of more parallel-fibered bone tissue with osteocyte lacunae arranged in parallel (ICL); a thick middle region of more woven-textured bone tissue with haphazardly organized osteocyte lacunae; and an outer region (OCL) of more parallel-fibered bone tissue with osteocyte lacunae that are flatter and arranged in parallel (SFig. 10A). The outer region is marked by several rest lines (estimated four). The middle region of the compacta is not as richly vascularized as in *Jeholornis*; isolated secondary osteons are visible, although fewer than observed in *Jeholornis*. The inner and medial regions are separated by an uneven tide line, clearly visible in polarized light, representing where resorption occurred before the inner layer was deposited. A LAG is found near the boundary between the OCL and the rapid growth region. The medullary surface is broken and no medullary bone can be identified.

Femur. Although less clear due to poor preservation, the thin section of the enantiornithine femur (SFig. 10B) displays three regions, as in the other sections: an inner poorly vascularized region of more parallel-fibered bone tissue with osteocyte lacunae arranged in parallel (ICL); a very thick middle region of more woven-textured bone tissue with haphazardly organized osteocyte lacunae; and a thin outer region (OCL) of more parallel-fibered bone tissue. The middle region accounts for most of the preserved thickness of the compacta; it is poorly vascularized with only a few longitudinal canals and interrupted roughly in the middle by a double LAG. Almost all the preserved secondary osteons are limited to the inner half of the middle region. Osteocyte lacunae are not visible in the OCL, which is marked by several rest lines (estimated four –five). The ICL and the medullary cavity are either poorly preserved or broken along the entire section; an uneven tide line separates the ICL from the middle region.

Discussion

Medullary bone is unique to egg-laying females, present in modern birds (including the ostrich with its proportionately small egg), and reported in a specimen of *T. rex* and several other dinosaurs[16] including one Mesozoic bird, *Confuciusornis sanctus*[36]. It forms in response to estrogen produced in the body during vitellogenesis, and provides a source of calcium for eggshell production. We conducted histological analysis of the three Mesozoic birds to further validate our interpretations of the follicular structures. Unfortunately, no medullary bone was preserved – however, because of the poor quality of the preserved bone, its absence may be taphonomic and the results are inconclusive. Medullary bone is extremely vascularized and could have been easily destroyed by crushing. Furthermore, egg-laying crocodilians do not form medullary bone[17] and thus its absence in a specimen could indicate a lower metabolic rate. The persistence of medullary bone varies among extant birds; its absence in a specimen may also indicate the female died before the formation of the medullary bone.

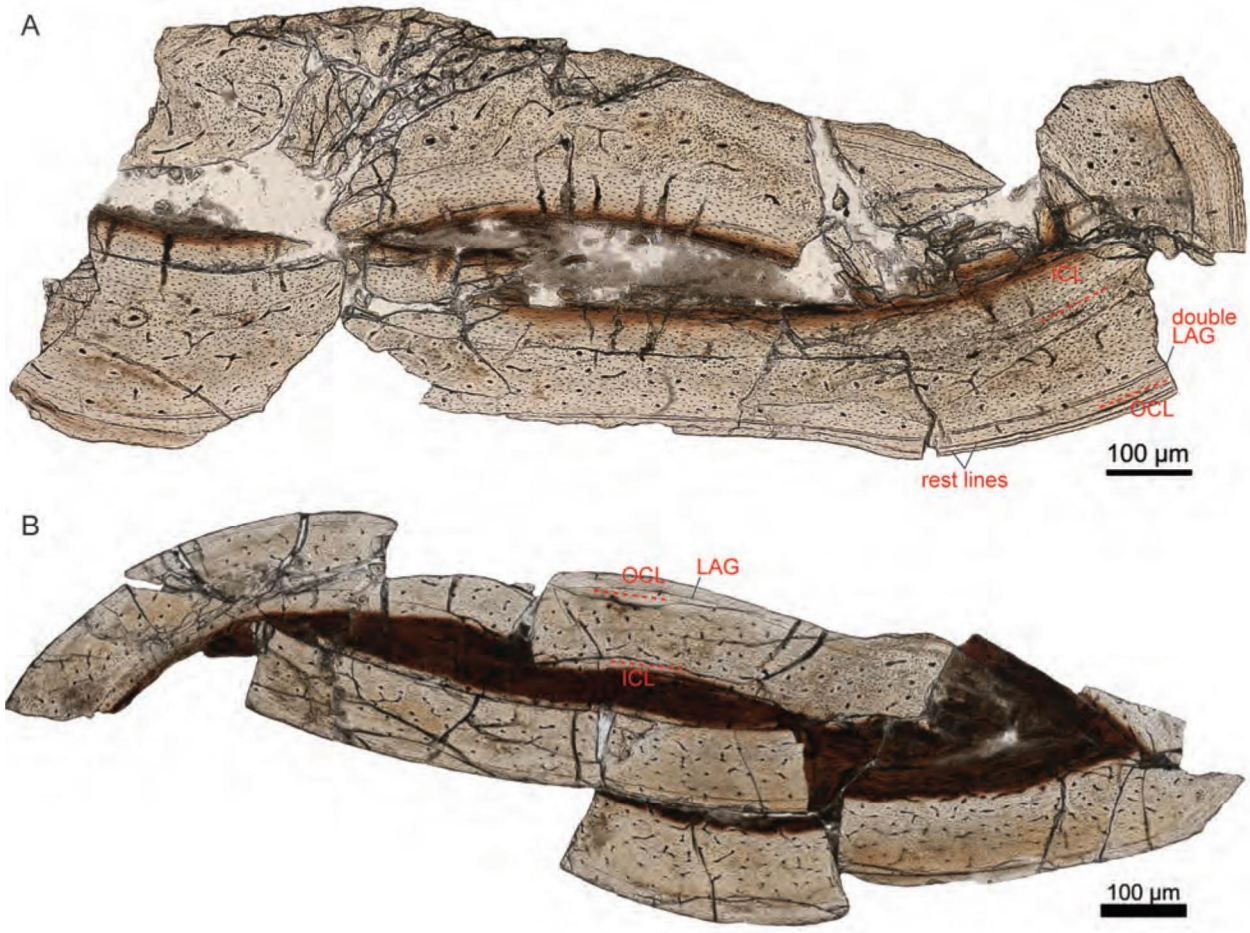

Figure S9. Histological thin sections from *Jeholornis* sp. STM2-51: A, ulna; B, femur. OCL, outer circumferential layer; ICL, inner circumferential layer.

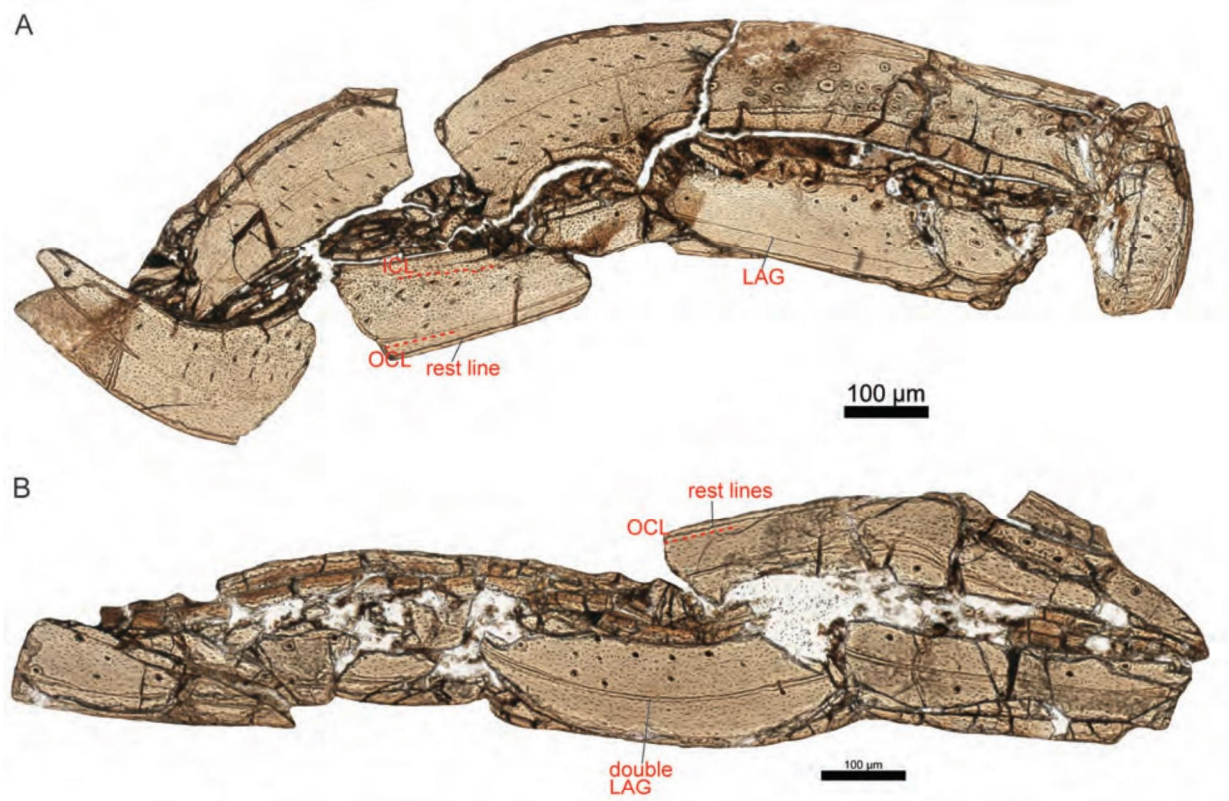

Figure S10. Histological thin sections from Enantiornithine sp. STM29-8: A, humerus; B, femur. OCL, outer circumferential layer; ICL, inner circumferential layer.

7. Supplementary References

[30]Benton, M.J., Zhou, Z.-H., Orr, P.J., Zhang, F.-C., & Kearns, S.L., The remarkable fossils from the Early Cretaceous Jehol Biota of China and how they have changed our knowledge of Mesozoic life: Presidential Address, delievered 2nd May 2008. *Proc Geol Assoc* **119** (3-4), 209-228 (2008).

[31]Allison, P.A., The role of anoxia in the decay and mineralization of proteinaceous macro-fossils. *Paleobiology* **14** (2), 139-154 (1988).

[32]Briggs, D.E.G., Wilby, P.R., Perez-Moreno, B., Sanz, J.L., & Frenegal-Martinez, M., The mineralization of dinosaur soft tissue in the Lower Cretaceous of Las Hoyas, Spain. *Journal of the Geological Society of London* **154** (4), 587-588 (1997).

[33]Dal Sasso, C. & Signore, M., Exceptional soft-tissue preservation in a theropod dinosaur from Italy. *Nature* **392**, 383-387 (1998).

[34]Briggs, D.E.G., The role of decay and mineralization in the preservation of soft-bodied fossils. *Annual Review of Earth and Planetary Science* **31**, 275-301 (2003).

[35]Tickle, P.G., Ennos, A.R., Lennox, L.E., Perry, S.F., & Codd, J.R., Functional significance of the uncinate processes in birds. *J Exp Biol* **210** (22), 3955-3961 (2007).

[36]Chinsamy, A., Chiappe, L.M., Marugán-Lobón, J., Gao, C.-H., & Zhang, F.-J., Gender identification of the Mesozoic bird Confuciusornis sanctus. *Nature Communications* DOI: 10.1038/ncomms2377 (2013).

[37]Chinsamy, A., Rich, T., & Vickers-Rich, P., Polar dinosaur bone histology. *J Vertebr Paleontol* **18** (2), 385-390 (1998).

[38]Liao, W.-B. & Lu, X., Age structure and body size of the Chuanxi Tree Frog *Hyla annectans chuanxiensis* from two different elevations in Sichuan (China). *Zool Anz* **248**, 255-263 (2010).